Calcif Tissue Int (2005) 76:261–271
DOI: 10.1007/s00223-004-0238-2

Calcified Tissue International

Laboratory Investigations

Osteoblast Responses One Hour After Load-Induced Fluid Flow in a Three-Dimensional Porous Matrix

Shigeo M. Tanaka,[1,2] Hui B. Sun,[2,5] Ryan K. Roeder,[4] David B. Burr,[2,3,5] Charles H. Turner,[3,5] Hiroki Yokota[2,5]

[1]Graduate School of Natural Science and Technology, Kanazawa University, Kanazawa, Japan
[2]Department of Anatomy and Cell Biology, Indiana University School of Medicine, Indianapolis, IN, USA
[3]Department of Orthopedic Surgery, Indiana University School of Medicine, Indianapolis, IN, USA
[4]Department of Aerospace and Mechanical Engineering, University of Notre Dame, Notre Dame, IN, USA
[5]Department of Biomedical Engineering, Indiana University–Purdue University, Indianapolis, IN, USA

Received: 30 September 2004 / Accepted: 7 October 2004 / Online publication: 11 April 2005

Abstract. When bone is loaded, substrate strain is generated by the external force and this strain induces fluid flow that creates fluid shear stress on bone cells. Our current understanding of load-driven gene regulation of osteoblasts is based primarily on *in vitro* studies on planer two-dimensional tissue culture substrates. However, differences between a flat layer of cells and cells in 3-dimensional (3D) ECM are being recognized for signal transduction. Proliferation and differentiation of osteoblasts are affected by substrate geometry. Here we developed a novel 3D culture system that would mimic physiologically relevant substrate strain as well as strain-induced fluid flow in a 3D porous collagen matrix. The system allowed us to evaluate the responses of osteoblasts in a 3D stress-strain environment similar to a mechanical field to which bone is exposed. Using MC3T3-E1 osteoblasts grown in the 3D collagen matrix with and without hydroxyapatite deposition, we tested the role of strain and the strain-induced fluid flow in the expression of the load-responsive genes such as c-fos, egr1, cox2, osteopontin, and mmp1B involved in transcriptional regulation, osteogenesis, and rearrangement of ECM. Strain-induced fluid flow was visualized with a microspheres ~3 μm in diameter in real time, and three viscoelastic parameters were determined. The results obtained by semi-quantitative PCR, immunoblot assay, enzymatic activity assays for collagenase and gelatinase, and mechanical characterization of collagen matrices supported the dominant role of strain-induced fluid flow in expression of the selected genes one hour after the mechanical treatment.

Key words: Bone — Osteoblasts — Mechanical loading — Fluid flow shear — Collagen matrix — Hydroxyapatite

Connective tissue cells such as chondrocytes, osteoblasts, and osteocytes alter gene expression in response to mechanical loads [1–3], but alteration of mRNA and protein levels as well as enzyme activities differs depending on loading conditions such as stress elements (tensile/compressive vs. fluid shear), intensity and duration [4]. In order to understand the role of mechanical stimuli in cellular proliferation and differentiation or to engineer functional scaffolds under mechanical loading, simulating a 3D *in vivo* stress-strain environment with a physiologically relevant extracellular matrix (ECM) substrate is important [5]. For instance, it is reported that 3D-matrix adhesions differ from focal and fibrillar adhesions characterized on 2D substrates [6], and the expression of matrix metalloproteinases (MMPs) is affected by the dimensionality of ECM [7].

Osteoblasts in bone are exposed to a complex stress-strain field in calcium-deposited ECM [8]. In response to mechanical loading, a highly networked collagen substrate receives not only normal (tensile/compressive) stress and strain but also fluid shear stress and strain in a porous matrix [9, 10]. Although the effects of substrate strain, fluid shear stress, or dissipation energy have been examined separately mostly using 2D substrates [4], it is difficult to evaluate the contribution of each mechanical input with mechanical loaders that are unable to induce substrate strain and fluid shear simultaneously. In this study, a novel 3D culture system utilizing a mechanical loader driven by piezoelectric actuators [11] was developed to simulate the 3D mechanical stress-strain environment in bone.

A specific question addressed here was whether MC3T3-E1 osteoblasts in a 3D collagen matrix would be most sensitive to substrate strain, strain-induced fluid flow, or viscoelastic energy dissipated in the ECM substrates. No studies have examined the effects of substrate stress/strain together with fluid-induced sheaf stress/strain in any 3D loading system. In our 3D

Correspondence to: Hiroki Yokota; E-mail: hyokota@iupui.edu

loading system, tubular collagen pores in the substrate mimic the networked microstructures in bone, and oscillatory strain induces dynamic fluid flow along the tubular pores. Coating a surface of porous matrices with a solidified collagen gel enabled us to simulate application of substrate stress/strain alone without inducing fluid flow across the matrix surface. An eddy-current displacement sensor allowed us to determine dissipation energy in the substrate in the presence and absence of fluid flow. It is therefore possible to differentiate the contribution of the ECM substrates to dissipation energy from the contribution of load-induced fluid flow. In order to evaluate the effects of calcium-deposited ECM in bone, hydroxyapatite (HA) was deposited to collagen matrices [12]. Based on the strain waveforms measured in dogs during walking [13, 14], an oscillatory compressive loading at 1 Hz with a peak-to-peak magnitude of 3000 μstrain was chosen as an input.

To address the question of responsiveness to varying mechanical stimuli, semi-quantitative PCR was conducted and the mRNA levels of stress-responsive genes such as c-fos, egr1, cox2, osteopontin, and mmp1B were evaluated. C-fos and egr1 are transcription factors responsive to varying chemical and biophysical stimuli, and they are involved in transcriptional regulation of many matrix proteins and MMPs [15]. Expression of cox2 and release of prostaglandin E_2 are linked to mechanically induced bone formation, and osteopontin (bone sialoprotein) is shown to be responsive to fluid shear in 2D cell cultures [4, 16]. Mmp1B is a collagenase involved in rearrangement of ECM and its expression is sensitive to mechanical strain and fluid flow [17, 18]. Mechanical characterization of the collagen matrices was also performed and three viscoelastic parameters — apparent elastic modulus, phase shift angles, and dissipation energy — were determined [19]. Scanning electron microscopy (SEM) and X-ray diffraction (XRD) revealed porous crystalline microstructures of the HA-deposited matrix. In response to sinusoidal strain at 1 Hz, strain-induced fluid flow was visualized in real-time. The results of PCR, immunoblot assay, protein activity assays and mechanical characterization of the collagen matrices supported the fact that substrate strain-induced fluid flow was more effective in the observed alteration in the mRNA and protein levels than substrate stress and strain or viscoelastic energy dissipated in collagen matrices.

Materials and Methods

Matrix Preparation and Cell Culture

3D porous collagen matrices (CollaCote, Centerpulse Dental, CA, USA) with coarse pores (mean ± SD; 89 ± 28 μm) and fine pores (22 + 7 μm) were used in the study. These matrices were cut in a dimension of 20 mm (width) × 16 mm (length) × 2 mm (thickness). Approximately 1×10^6 of MC3T3-E1 osteoblast cells at a passage number of ~ 18 were seeded in the 3D matrix with 3 ml α-MEM culture medium (Sigma, MO, USA) consisting of 10% FBS and antibiotics (0.05 U/ml penicillin and 0.05 μg/ml streptomycin). Prior to application of mechanical stimuli, cells were incubated in the matrix for 3 hours at 37°C.

Deposition of Hydroxyapatite (HA) for Porous Collagen Matrix

The microstructure of porous collagen matrices with coarse pores was modulated by deposition of a varying amount of HA. The matrix was soaked in a 500-mM $CaCl_2$ solution followed by a 500-mM Na_2HPO_4 solution for 15 min each. The matrix was thoroughly rinsed in sterile water between immersions, and alternate immersion in $CaCl_2$ and Na_2HPO_4 solutions was repeated twice (2-cycle deposition) or four times (4-cycle deposition). After this HA deposition, the matrices were rinsed in sterile water five times and then rinsed in the medium five times. By rising, pH of the medium in the matrix was maintained at ~ pH 7.4. The HA-treated matrix was used immediately after the rising for the loading experiment. To evaluate the amount of HA deposition, a dry weight of matrices was measured and the change in matrix mineralization was identified by von Kossa staining.

SEM

Matrix morphology was analyzed using a scanning electron microscope (Amray 1000 A, KLA-Tencor, MA, USA), operated at 20 kV. The matrix sample was fixed with 1% osmium tetroxide, and dehydrated in a series of graded alcohols. The sample was then dried using a critical point dryer (Samdri-780, Tousimis Research Corp., MD, USA), and coated with gold palladium using sputter deposition (Hummer V, Anatech LTD., VA, USA). The pore sizes were determined from the SEM images.

XRD

In order to identify crystalline phases, the surface of dried collagen matrices was analyzed by x-ray diffraction (X1, Advanced Diffraction System, Scintag, Inc., USA) using Cu Kα radiation generated at 45 kV and 40 mA. Specimens were examined over 10–60° two theta with a step size of 0.02° and step time of 1.0 sec. Diffraction peaks were identified relative to known standards.

Histology

Osteoblasts in the porous collagen matrix were fixed in a 100-mM cacodylate buffer containing 2% paraformaldehyde and 2% glutaraldehyde, and the fixed sample was dehydrated in a series of graded alcohols. The sample was then embedded in paraffin and cut into 5-μm sections. The section of the control matrix and the HA-deposited matrix was strained with a Hematoxylin-Eosin (H + E) or MacNeal's tetrachrome, respectively, for analyzing the distribution of osteoblasts and the calcified regions, respectively.

Mechanical Loading

Cells grown in the 3D porous collagen matrix were subjected to oscillatory strain for 3 min with a piezoelectric mechanical loader [9]. The strain wave was sinusoidal at 1-Hz with a magnitude of 0–3,000 μstrain (0.3% compressive deformation). The applied strain generated oscillatory fluid flow at 1 Hz in the porous collagen matrix. To evaluate the effects of strain alone without induction of fluid flow (strain control), a surface

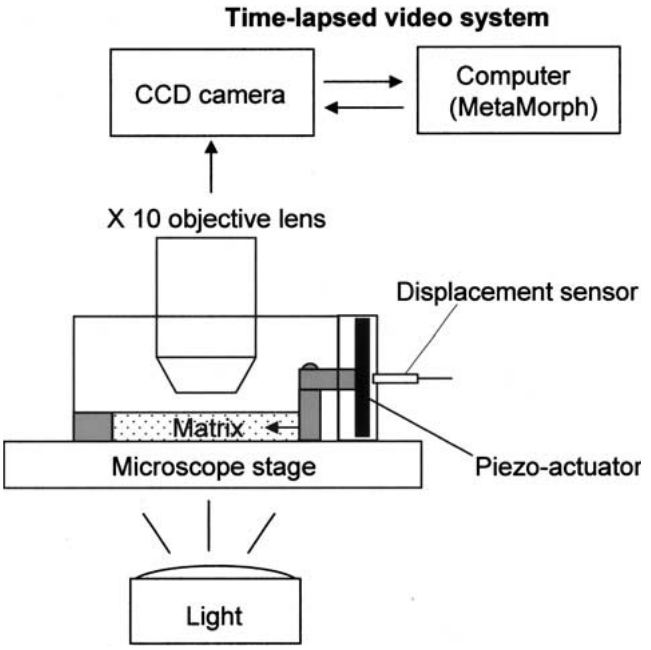

Fig. 1. Visualization of strain-induced fluid flow. Polystyrene microspheres (3 μm in diameter) were seeded with the culture medium into a porous collagen matrix placed in the mechanical loader on the stage of an inverted microscope (for the gel-covered matrix, the matrix was covered by a collagen gel after the seeding of the microspheres). Sinusoidal compressive strain at 1-Hz with a magnitude of 0–3,000 μstrain was applied to the matrix and induced fluid flow in the matrix. The motion of microsphears representing the motion of strain-induced fluid flow was captured through a 10× objective lens at 250 msec interval by a time-lapsed video system.

of matrices was covered with a collagen gel that prevented fluid flow across the matrix surface. A collagen solution at a concentration of 1 mg/ml (BD Biosciences, NJ, USA) in α-MEM (Sigma, MO, USA) was warmed up to 22°C and put on a matrix, making all surfaces of the matrix wrapped by the solution except two surfaces loaded by the loading device. After incubation at 37°C for 30 min, the surfaces of matrix were covered by collagen gel like a sheet (∼ 0.5 mm thick). In the gel-covered matrix, no detectable internal pressure change in response to mechanical strain was observed at a resolution of 0.5 mmHg using a fiber-optic pressure transducer (FOP-MIV, Fiso Technologies Inc., Quebec, Canada).

Visualization of Strain-induced Fluid Flow

Strain-induced fluid flow was visualized through the motion of polystyrene microspheres, approximately 3 μm in diameter (Polysciences, Inc., PA, USA). Time-elapsed images were taken at 250-msec intervals using a Nikon E600 microscope with a 10× objective lens. Four images per cycle (1 Hz) were captured and analyzed using MetaMorph software (version 3.6, Universal Imaging Co., PA, USA) (Fig. 1).

Measurement of Viscoelastic Properties

To determine the viscoelastic properties such as apparent elastic modulus, phase shift angle, and dissipation energy, a force-sensing module was attached to the piezoelectric loader. The module measured the force applied to the matrix at a resolution of 50 μN by detecting deflection of the cantilever connected to the matrix. In response to a compressive sinusoidal strain at 1 Hz with a magnitude of 3000 μstrain, stress in the matrix was estimated from the measured force and a cross-sectional area of the matrix. Apparent elastic modulus was determined as an average slope in the strain-stress relationship. A phase shift angle, an indicator of viscosity, was calculated as a phase difference between the measured force and the applied strain using a Fourier analysis. Dissipation energy was determined numerically by integrating an area inside a hysteresis loop in the stress-strain relationship.

Semi-Quantitative RT-PCR

The mRNA level of the selected genes such as c-fos, egr1, cox2, osteopontin (opn), and matrix metalloproteinase-1B (mmp1B) was determined by semi-quantitative RT-PCR using a pair of specific PCR primers (Table 1). The selected genes are known as load-sensitive genes in several types of cells [20–23]. C-fos and egr1 are transcription factors, cox2 and opn are upregulated in load-driven bone adaptation. Mmp1B is a collagenase that plays the role in growth and rearrangement of extracellular matrix. One hour after mechanical stimuli, the matrices were removed from the loading chamber and homogenized immediately in a lysis buffer. Total RNA was extracted using RNaeasy minikits (Qiagen Inc., CA, USA), and the isolated RNA was reverse-transcribed as described previously [24]. The reverse-transcribed cDNA was amplified using a thermal cycler (Gene-Amp PCR system 2400, Perkin Elmer, CT, USA) for 30 cycles (94°C for 1 min, 54–58°C for 30 sec, and 72°C for 30 sec). By adjusting the amount of total RNA before PCR, all PCR-products were amplified linearly around 30 cycles. PCR products were electrophoresed on 1.2% agarose gel, and visualized by ethidium bromide. The intensity of electrophoretic bands was quantified using PhotoShop (Adobe Systems Inc., CA, USA). Glyceraldehyde-3-phosphate dehydrogenase (gapdh) was used as RT-PCR control, and RT-PCR was conducted three times.

Immunoblot Assay

An immunoblot assay was performed by using antibody specific for Cox-2 (Santa CruzBiotechnology, NY, USA). One hour after mechanical stimuli, culture cells were harvested in the cell lysis buffer containing 20 mM Tris (pH 7.5), 150 mM NaCl, 1 mM EDTA, 1 mM EGTA, 1% Triton X-100, 2.5 mM sodium pyrophosphate, 1 mM beta-glycereolphosphate, 1 mM Na_3VO_4, 1 μg/ml leupeptin and 1 mM PMSF. Approximately 10 mg of the extracted proteins were separated by electrophoresis (SDS-PAGE) in a polyacrylamide gel, and the separated proteins were transferred to nitrocellulose membranes (Hybond, Amersham, NJ, USA). Membrane was incubated with primary antibodies followed by incubation with secondary antibodies conjugated to horseradish peroxidase (ECL Western Blotting analysis system, Amersham, NJ, USA). The expected molecular size for Cox-2 is 72 kDa. A mouse antibody specific for β-actin (42 kDa, Sigma, MO, USA) was used as loading control.

Collagenase and Gelatinase Activity Assay

The total enzyme activities of collagenases including the activities of MMP1, MMP8 and MMP13, and the total enzyme activities of gelatinases including the activities of MMP2 and MMP9 were determined by fibril degradation assay using Enzcheck Collagenase/Gelatinases Assay Kit (Molecular Probes, OR, USA). The proteins isolated from the culture media one hour after mechanical stimuli were incubated with fluorescent substrates in a reaction buffer consisting of 50 mM Tris-HCl (pH 7.6), 150 mM NaCl, 5 mM $CaCl_2$, and 0.2 mM sodium azide at room temperature for 2 hours. Fluorescent intensity, a measure of enzyme activity, was determined by a FluroMax-2 spectroflurometer (Instruments S.A., Inc., CA,

Table 1. Primers for semi-quantitative PCR

Gene	Sense primer	Antisense primer	Size (bp)
c-fos	5′-CGTTGCAGACTGAGATTGCC-3′	5′-GCTCCAGCTCTGTGACCATG-3′	432
egr1	5′-GCCTAGTCAGTGGCCTCGTG-3′	5′-ACTGCAAGGCTGTGCCTGCC-3′	374
cox2	5′-ATGACATCGATGCCATGGAA-3′	5′-TCAGTAGACTCTTACAGCT-3′	382
opn	5′-CCAACGGCCGACCTGATAG-3′	5′-CACTACCTTATTGCCCTCCTGC-3′	343
mmp1B	5′-GTGATTCAGGATGGACTCCAG-3′	5′-TCGCGATGGCATCTTCCACAA-3′	240
gapdh	5′-GCCACCCAGAAGACTGTGGAT-3′	5′-TGGTCCAGCCTTTCTTACTCC-3′	477

USA). An absorption/emission wavelength was set to 495/515 nm. The culture medium itself exhibited basal collagenase activity and gelatinase activity that was ~5% of that in the medium incubated with control cells.

Statistical Methods

Analysis of variance was conducted to examine statistical significance in alteration of the viscoelastic properties of the matrix and the mRNA level of the load-sensitive genes. Fisher's PLSD (Protected Least Significant Difference) tests were performed to evaluate differences among pairs of samples (Starview, SAS Institute, NC, USA). *P*-values less than 0.05 were considered statistically significant.

Results

Deposition of Hydroxyapatite (HA) to Collagen Matrix

In the current studies, the molecular responses to mechanical loading were investigated using MC3T3-E1 osteoblasts grown in 3D collagen matrix with and without HA deposition. The microstructure of porous collagen matrices with coarse pores was modulated by alternate immersion in $CaCl_2$ and Na_2HPO_4 solutions. SEM photomicrographs clearly showed that soaking in these solutions altered porosity of the matrices and reduced the pore size (Fig. 2A). The mean diameter (± SD) of tubular pores, measured from the SEM images, was 89 ± 28 μm (no HA deposition), 56 ± 12 μm (2-cycle HA deposition), and 25 ± 10 μm (4-cycle HA deposition). A dry weight of matrices was increased by 0.44 mg and 1.79 mg by 2-cycle and 4-cycle deposition, respectively. In concert with the dry weight measurement, the intensity of von Kossa staining was elevated by HA deposition (Fig. 2B). X-ray diffraction of HA deposited matrices revealed characteristic peaks corresponding to HA (Fig. 2C) ([12], Powder Diffraction File 05-0418, "$Ca_5(PO_4)_3(OH)$," JCPDS-ICDD, 1997.). The broad diffraction peaks for HA were indicative of nano-sized crystallites, similar to that measured for human bone mineral. The control matrix (no HA deposition) displayed no diffraction peaks characteristic to crystalline phases.

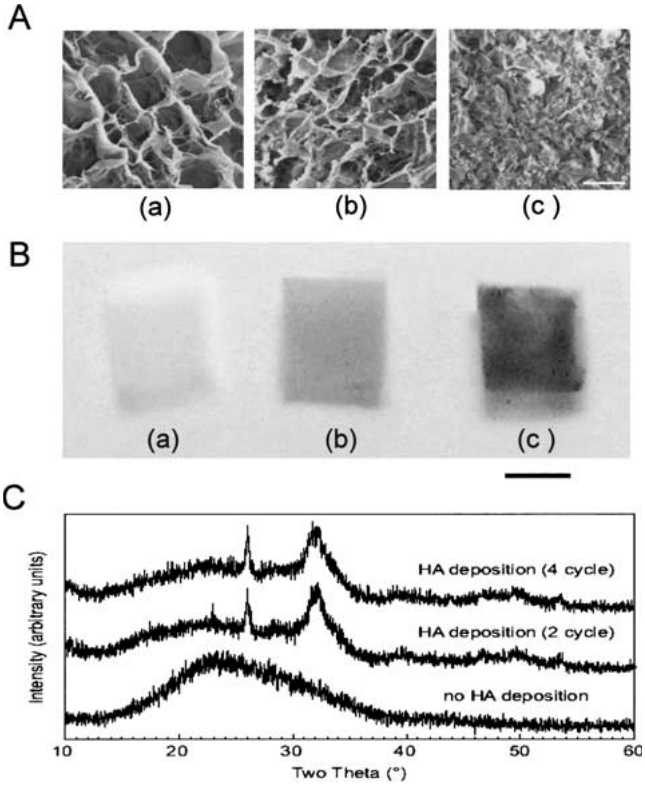

Fig. 2. Deposition of hydroxyapatite (HA) in a porous collagen matrix. (**A**) SEM photomicrographs of the matrices. (**a**) Control collagen matrix without HA deposition; (**b**) HA-deposited collagen matrix (2 cycles of deposition); and (**c**) HA-deposited collagen matrix (4 cycles of deposition). The white bar represents 100 μm. (**B**) von Kossa staining of the matrices. The black bar indicates 5 mm: (**a**) no HA deposition; (**b**) HA deposition (2 cycles); and (**c**) HA deposition (4 cycles). (**C**) X-ray diffraction patterns for the control matrix (no HA deposition) and the HA-deposited matrices (2 and 4 cycles of deposition). The spectral peak at 32° is characteristic of HA.

Cellular Morphology in Collagen Matrix

Osteoblasts were grown in the collagen matrix with and without HA deposition. In a control matrix without HA deposition, H + E staining showed that osteoblasts were apparently able to anchor and extend their fibrous microstructure in the 3D porous matrix 24 hours after the seeding (Fig. 3A). In the HA-deposited matrix, MacNeal staining revealed that many cells were positioned in the vicinity of the calcified regions (Fig. 3B). The image was taken from the center section, 1 mm in depth from a surface of the collagen matrix. Although cells were spread in the matrix, ~30% more cells were located on the outer half sections of the matrix than the inner half sections.

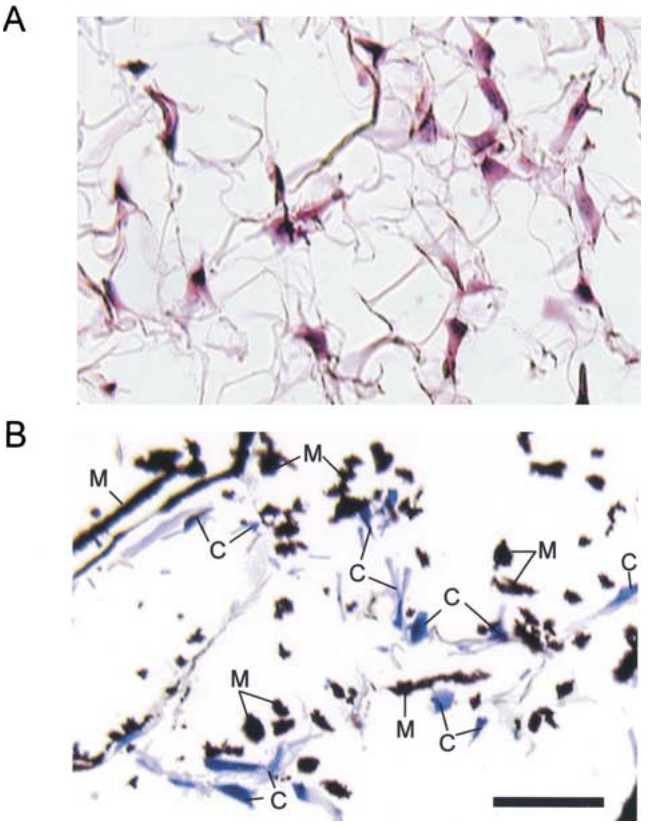

Fig. 3. MC3T3-E1 cells cultured in the porous collagen matrix. Cells were grown in the matrices for 24 hours after seeding. The bar is 100 μm. (**A**) Hematoxylin-eosin stained cells in a control collagen matrix. (**B**) MacNeal-stained cells in a HA-deposited (4 cycles) collagen matrix. The HA-deposited matrix and cells were stained black and blue by MacNeal staining, and marked with "M" and "C," respectively.

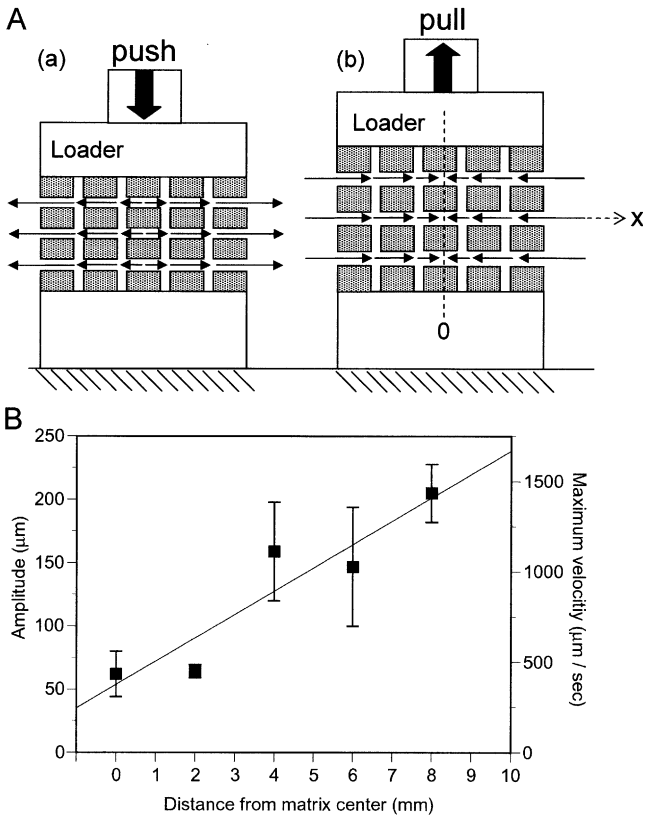

Fig. 4. (**A**) A schematic diagram of strain-induced fluid flow in the porous collagen matrix. (**a**) compressed porous matrix (represented by the shaded rectangles) with a fluid flow moving outwards; and (**b**) stretched matrix with a fluid flow moving towards a neutral plane (matrix center indicated by a vertical dashed line). (**B**) Distribution of amplitudes and maximum velocities of the microspheres in the fluid flow induced by sinusoidal strain at 1 Hz with 3000 μstrain (peak-to-peak). The matrix was deposited with HA (4 cycles). The bar represents the mean ± SE of five measurements. The maximum velocity (Vmax) was estimated from the measured amplitude using the following formula: Vmax = $2\pi f \times$ (peak-to-peak amplitude)/2, where f is the frequency.

Modulation of Strain-Induced Fluid Flow

In the current study, fluid flow was induced by controlled deformation of 3D substrates (Fig. 4A). In the porous 3D collagen matrix, position (travel amplitude) and velocity of strain-induced fluid flow were determined with the microspheres. In response to sinusoidal strain at 1 Hz (3000 μstrain) in the matrix with fine pores, the motion of fluid flow was correlated to the distance from the neutral plane of the matrix (matrix center) (Fig. 4B). The best-fit regression line for amplitude, y (μm), was

$$y = 18x + 54 \text{ with } r^2 = 0.89,$$

where x (μm) represented distance from the matrix center along the x-axis.

Compared to fluid flow in the matrix with coarse pores, the flow amplitude and velocity were elevated in the matrix with fine pores as well as in the matrix with HA deposition (Fig. 5). In all matrices, a flow direction was aligned to the local tubular pores. A majority of cylindrical pores ran parallel to the x-axis, and strain-induced fluid flow was organized as shown in Figure 4A. The amplitude and the maximum velocity were 15.6 μm and 98 μm/sec (coarse-pored matrix), 76.9 μm and 483 μm/sec (fine-pored matrix), and 138 μm and 867 μm/sec (HA-deposited matrix; 4-cycle deposition) (Fig. 5B). No motion of the microspheres was observed in the matrix covered with collagen gel (strain control).

Viscoelastic Properties of the Matrix

In response to sinusoidal loading at 1 Hz, three viscoelastic parameters – apparent elastic modulus, a phase shift angle, and dissipation energy – were measured for the three different matrices in the presence and absence of gel covering. Apparent elastic modulus was increased 60-fold by HA deposition, and covering a matrix with

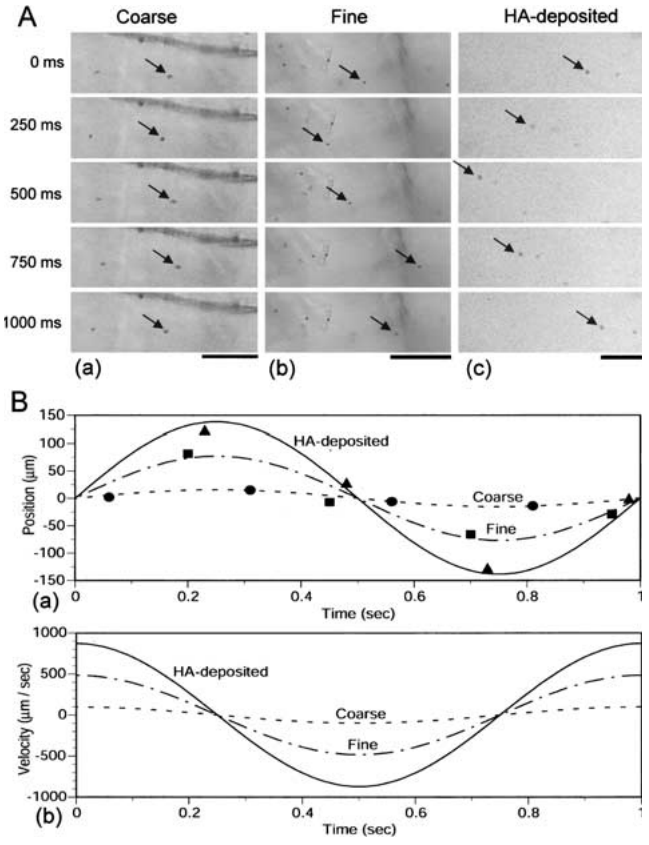

Fig. 5. (**A**) Time-elapsed image of the microspheres in strain-induced flow. Sinusoidal compressive strain with a magnitude of 0–3,000 μstrain was applied at 1 Hz. The black arrows point to a moving microsphere, approximately 3 μm in diameter, which was located at ~5 mm from the neutral plane of the matrix (x = 5 mm). The scale bars are 100 μm. (**a**) Flow in the matrix with coarse pores; (**b**) flow in the matrix with fine pores; and (**c**) flow in the HA-deposited matrix (4 cycles). (**B**) Position and estimated velocity of the microspheres: (**a**) position of the microspheres. The symbols (triangles, square, and circles) represent the images in Figs. **4A-(a)**, **4A-(b)**, and **4A-(c)**, respectively. Three regression curves in μm are *15.6 sin2πt* (4A-(a)), *76.9 sin2πt* (4A-(b)), and *138 sin2πt* (4A-(c)); and (**b**) estimated velocity of the microspheres by differentiating the position with respect to time.

gel elevated the modulus 1.8-fold (nondeposition) and 1.4-fold (HA deposition) (Fig. 6A). A phase shift angle was decreased 0.4 fold by HA deposition, but increased 1.3-fold (no deposition) and 1.5 fold (HA deposition) by gel covering (Fig. 6B). Dissipation energy was increased 20 fold by HA deposition, and gel covering increased the energy 2.4 fold (no deposition) and 2.1 fold (HA deposition) (Fig. 6C). To summarize, (i) no significant differences were observed between the coarse-pored and the fine-pored matrices; (ii) the matrix with HA deposition showed higher elastic modulus and dissipation energy, and a lower phase shift angle than the matrix without HA deposition; and (iii) gel covering increased the three parameters in all matrices.

Alteration in mRNA Expression

Focusing on the mRNA expression of the selected load-responsive genes, the responses of MC3T3-E1 osteoblasts to sinusoidal strain, and strain plus strain-induced fluid flow, were examined in the matrix with coarse pores, fine pores, or HA deposition (4 cycles). The semi-quantitative PCR results showed that strain-induced fluid flow was a stronger stimulus than strain or dissipation energy in substrates to alter the mRNA expression level regardless of HA deposition (Fig. 7).

In the matrices without HA deposition, strain-induced fluid flow up-regulated the mRNA level of all five genes including c-fos, egr1, cox2, osteopontin, and mmp1B, and elevation was higher in the matrix with fine pores than that with coarse pores. Application of strain alone, on the other hand, elevated the level of c-fos mRNA and osteopontin mRNA but did not elevate the mRNA level of egr1, cox2, or mmp1B (Fig. 7A).

In the HA-deposited matrix (4 cycles), the basal mRNA expression of cox2 and mmp1B were detected. The expression of these two genes was significantly lower in the matrix without HA deposition in our PCR condition. As in the matrix without HA, the effects of strain-induced fluid flow on gene expression were stronger than strain alone (Fig. 7B). Fluid flow elevated the mRNA level of the five genes 2-fold or more compared to the no-loading control and the strain control. For strain alone in the HA constructs, stimulation of egr1 and opn were undetectable in our PCR conditions.

Alteration in Protein Expression and Activity

The protein production and activities from MC3T3-E1 osteoblasts after exposure to sinusoidal strain and strain plus strain-induced fluid flow were examined in the matrix with fine pores. Alteration of cox2-protein expression by the immunoblot assay showed that strain-induced fluid flow was a stronger stimulus than strain or dissipation energy in substrates. Cox2 protein was expressed more intensively by strain plus strain-induced fluid flow than by strain alone (Fig. 8A). Similarly, both collagenase and gelatinase activities were increased about 1.4-fold more with strain plus strain-induced fluid flow compared to strain alone (Fig. 8B).

Discussion

Many lines of evidence support the fact that bone formation is stimulated *in vivo* by strain [25–27] and strain-induced fluid flow [10, 28]. However, most *in vitro* studies so far have been directed to evaluating the effects of either strain of 2D substrates [29–31] or fluid flow that was not induced by deformation of ECM substrates [32, 35–35]. In this study, induction of fluid flow by well-

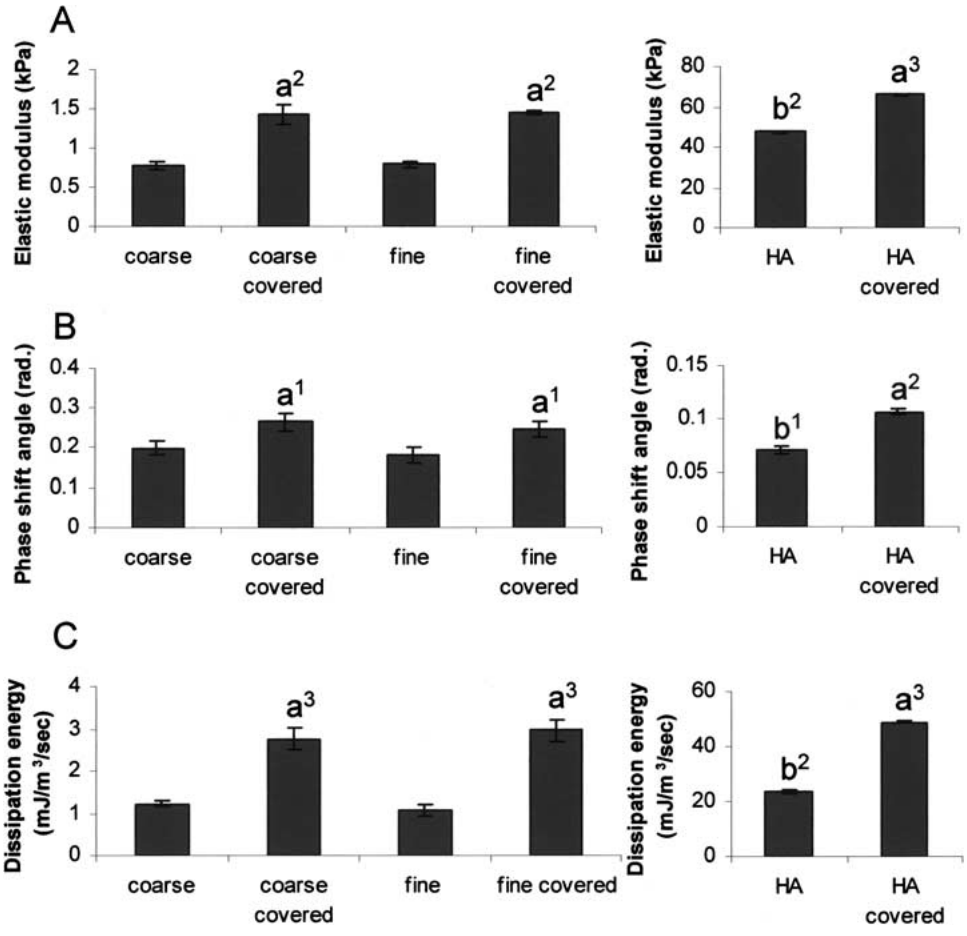

Fig. 6. Viscoelastic properties of the porous and gel-covered matrices in response to sinusoidal loading at 1 Hz. (**A**) Apparent elastic modulus, (**B**) phase shift angle, (**C**) dissipation energy. Three matrices with coarse pores (coarse), fine pores (fine), and 4-cycle HA deposition (**HA**) were characterized in the presence and absence of gel covering. The gel-covered matrices were used to remove the effects of strain-induced fluid flow. The measurements were performed on three samples. The bar represents the mean ± SE of three measurements. The symbols indicate statistical significance at $^{a1}P < 0.05$, $^{a2}P < 0.001$, and $^{a3}P < 0.0001$ versus the matrix without gel-covering, and at $^{b1}P < 0.05$ and $^{b2}P < 0.0001$ versus the matrix without HA deposition.

regulated deformation of 3D porous matrices was achieved for the first time with the newly developed mechanical loader. Its motion was feedback-controlled at ~50 nm resolution with the piezoelectric actuator and the eddy-current displacement sensor. Sinusoidal compressive loads at 1 Hz with a magnitude of 0–3,000 μstrain, used in this study, were based on the strain magnitude measured in dogs during walking [13, 14]. Using MC3T3-E1 osteoblast cells grown in the collagen matrix with and without HA deposition, we showed that strain-induced fluid flow was a more potent activator of expression and product of the load-responsive genes than substrate strain alone or dissipation energy in ECM substrates. This result implies the critical role of fluid-shear in mechanotransduction of osteoblasts. As candidates for potential shear-sensing mediators, Ca^{2+} channels [36] and membrane-bound receptors such as G-protein-linked receptors [37] have been suggested.

In the early responses of osteoblasts to strain-induced fluid flow, the altered expression of the selected five genes in the 3D matrix indicates involvement of multiple signal transduction pathways. In cultured osteoblasts grown on a flat substrate, extracellular-signal regulated kinase and p38 mitogen-activated protein kinase are reported to mediate induction of osteopontin in response to fluid shear [4]. Elevation of cox2 expression is dependent on the protein kinase A signaling pathway [16], but inhibition of cox2, does not affect load-driven activation of egr1 [38]. Fibronectin-induced formation of focal adhesions is shown to promote upregulation of cox2 in MC3T3-E1 cells grown on a 2D substrate. In 3D cell cultures, however, interactions between integrin and fibronectin are changed with a reduced level of tyrosine phosphorylation of focal adhesion kinases [39]. Furthermore, the basal expression level and the activation level of MMPs in 3D matrix are different from those in 2D culture [40]. A further study is needed to identify a complex network of mechanotransduction pathways and any effects of the dimensionality of substrates.

Although our results, obtained in the 3D porous matrix, support the previous findings in 2D substrates that osteoblasts are sensitive to fluid flow [20], we also expected to find a positive correlation between dissipation energy and osteoblastic response. In contrast to our expectation, covering the matrix with gel significantly increased the total amount of dissipation energy, but decreased osteoblastic response. Since the gel-covering decreased fluid flow, we conclude that the major contributor to dissipation energy in this *in vitro* system was not fluid flow. This observation was consistent in the

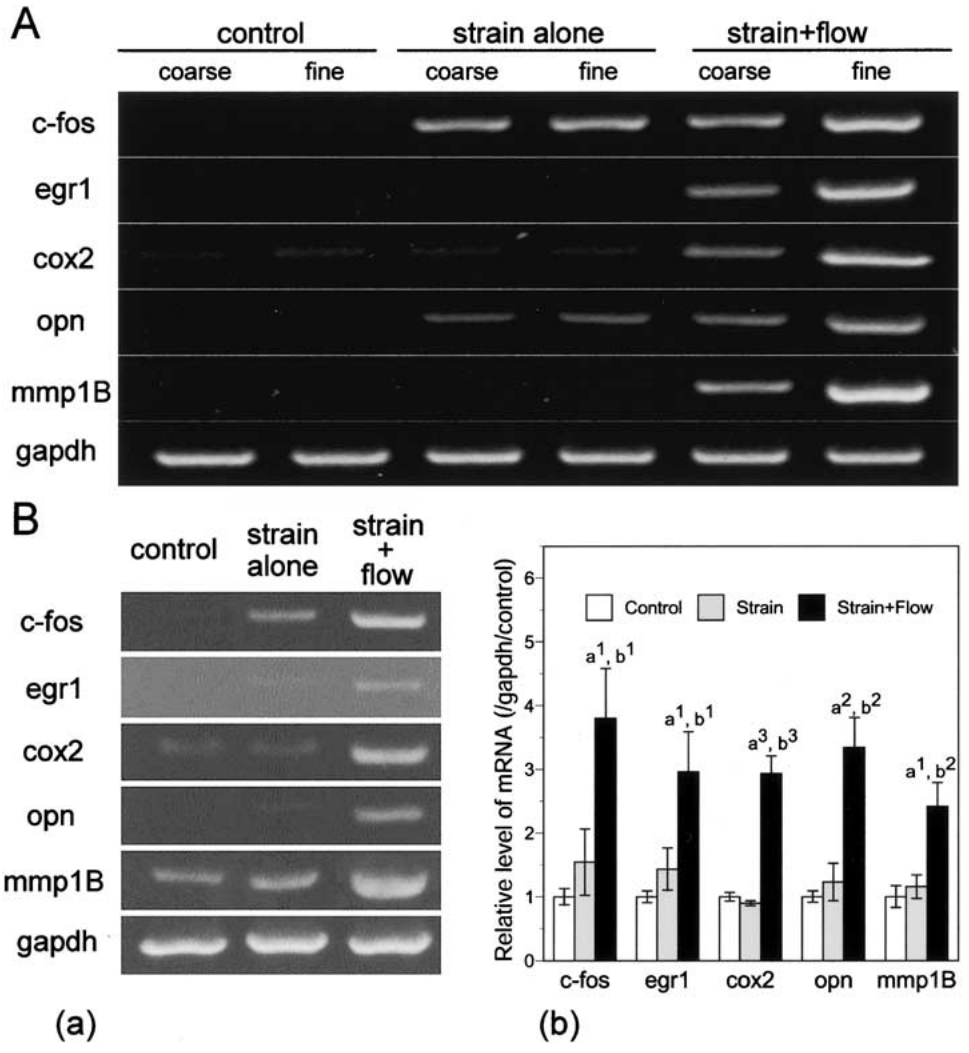

Fig. 7. Messenger RNA levels of c-fos, egr1, cox2, mmp1B, and osteopontin in response to mechanical stimuli in MC3T3-E1 cells. The gapdh level was used as control. Three mechanical conditions are "control" (no mechanical loading), "strain alone" (no fluid flow with gel-covered matrix), and "strain + flow" (strain and strain-induced flow). (**A**) Electrophoretic gel for the matrix with coarse pores ($d = 101 \pm 22$ μm) and fine pores ($d = 22 \pm 7$ μm). (**B**) Messenger RNA expression with the HA-deposited matrix (4 cycles), (**a**) Electrophoretic gel for the HA-deposited matrix; and (**b**) relative mRNA level to the control without mechanical stimuli for the HA-deposited matrix. The bar represents the mean ± SE of four measurements, and the symbols indicate statistical significance at $^{a1}P < 0.01$, $^{a2}P < 0.001$, and $^{a3}P < 0.001$ versus "control," and $^{b1}P < 0.05$, $^{b2}P < 0.01$, and $^{b3}P < 0.0001$ versus "strain alone."

three different matrices we used, i.e., coarse pores, fine pores, and HA deposition. Our results suggest that the observed increase in dissipation energy was due to viscoelastic deformation of the matrices and that dissipation energy is not associated with changes in mRNA levels of the selected load-sensitive genes.

Load-induced fluid shear in bone is estimated on the order of 1–10 dyn/cm^2 [41], although precise prediction varies depending on anatomical parameters as well as mathematical models. Monitoring the motion of the microspheres allowed us to estimate the velocity of fluid flow and flow-driven shear stress in matrices. In response to 3000-μstrain sinusoidal loads at 1 Hz, the flow speed of the microspheres was 867 μm/sec in the matrix with the HA-deposited matrix (4 cycles). In a simplified Poisseuille flow model for a cylindrical tube, shear stress, τ, on a pore surface can be estimated:

$$\tau = 4\mu Q/(\pi r^3),$$

where μ = viscosity (0.012 g/cm sec), Q = flow rate, and r = pore radius. Using r = 12.5 μm and assuming that Q is approximated by "cross-sectional area" times "flow speed," shear stress is estimated as ~ 3 dyn/cm^2. A more rigorous model of oscillatory flow in a porous matrix should consider variations in flow pattern in a finite matrix [42].

Deposition of hydroxyapatite to porous collagen matrices did not alter the mechanical responses of osteoblasts, in spite of the fact that HA stiffened the collagen matrix and increased energy dissipation in the calcified ECM. The mRNA expression level of the load-responsive genes was altered in a similar manner both in the HA-deposited matrix and the control matrix with fine pores. These two matrices generated comparable fluid flow in response to the same sinusoidal load (Fig. 5A), and the results support the fact that fluid flow is a critical signal for mechanotransduction.

One significant difference between the cells grown in the control matrix and the HA-deposited matrix was the basal expression level of cox2 and mmp1B. Even without exposure to loading, osteoblasts on the HA-deposited matrix exhibited a higher level of cox2 mRNA and

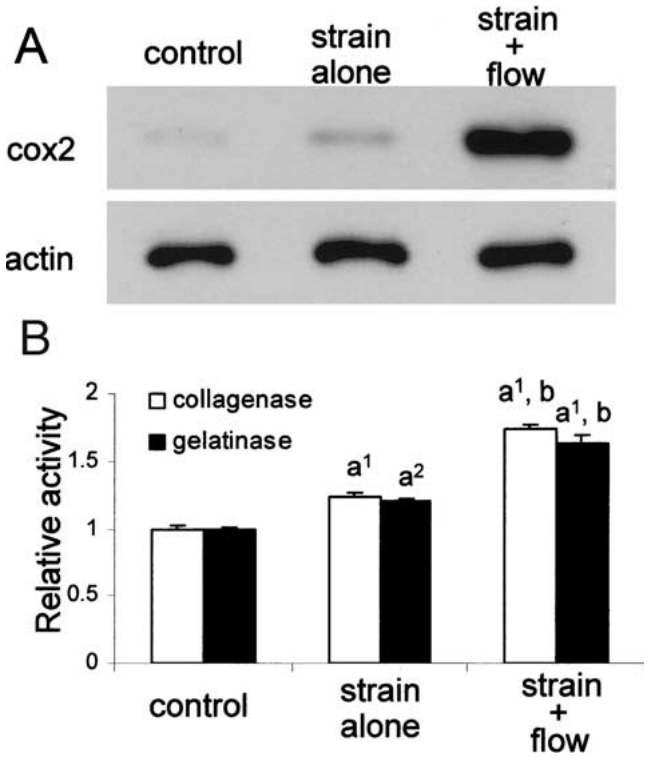

Fig. 8. (**A**) Protein level of cox2 in response to mechanical stimuli in MC3T3-E1 cells. The actin level was used as control. (**B**) Relative activity levels of collagenases and gelatinases in response to mechanical stimuli in MC3T3-E1 cells to the control. The cells were seeded in a collagen matrix with fine pores (d = 22 ± 7 μm). Three mechanical conditions are "control" (no mechanical loading), "strain alone" (no fluid flow with gel-covered matrix), and "strain + flow" (strain and strain-induced flow). The bar represents the mean ± SE of four measurements, and the symbols indicate statistical significance at $^{a1}P < 0.0001$, $^{a2}P < 0.001$ versus "control," and $^{b}P < 0.0001$ versus "strain alone."

mmp1B mRNA than those on the control matrix after four hours in culture. The results suggest that the calcium-deposited microstructure could alter osteoblastic phenotype in the absence of mechanical stimuli. It is reported that HA suppresses proliferation [43–46] and promotes differentiation [43, 45] and calcification of osteoblasts [47, 48]. However, the incubation time of 4 hours in the current study is not considered long enough to detect further alteration in gene expression caused by HA. Subtle differences in a chemical composition or a surface charge between our 3D system and the *in vivo* milieu might influence the effect of HA [49].

Although elevation of the mRNA level of osteopontin, collagen, and actin was reported in osteoblasts *in vitro* 1–8 days after intermittent hydrostatic compression at 13 kPa [47, 48], any increase in hydrostatic pressure or pressure-related alteration in gene regulation was not detected in the control cells grown in the gel-covered matrix. Our pressure measurement using the fiber-optic transducer with a resolution of 0.07 kPa showed no apparent pressure increase with or without the mechanical loading.

One limitation of the *in vitro* loading system in the current study is that the fluid channels in the 3D collagen matrix differ in size from channels in bone, i.e., the lacunocanalicular networks that are 10–100 nm in diameter. In a hierarchical nanostructure in bone *in vivo*, strain induced by external loads can be amplified by fluid flow in a nanometric scale [52]. In the SEM image, a collagen pore in our study appeared as a tubular cylinder confined in a thin wall-like column 10–100 μm in diameter. Although some of the ridges running parallel to the cylindrical pores were in a submicron scale, no tubular pores like those in a lacunocanalicular network were present in the ECM substrates we employed. Therefore, deviation of our 3D collagen matrices from *in vivo* structures must be noted in interpreting the present results.

The piezoelectric loader, described in this study, can be used to analyze gene expression in response to actual strain measured in animals and humans during daily exercises. Furthermore, the loader will be useful to grow cell-scaffold complexes and by selecting the parameters for mechanical loads. In conclusion, the loading system supported the fact that strain-induced fluid flow plays the dominant role in regulation of the selected genes one hour after the mechanical treatment in MC3T3-E1 osteoblasts compared to substrate stress and strain or viscoelastic energy dissipated in ECM substrates.

Acknowledgments. The authors appreciate Randall Duncan for cell cultures, Taffy Hooser for histology, Caroline Miller for SEM, and Razi Nalim and Kerem Pekkan for the flow analysis. This study was supported by The National Institutes of Health (R01EB001019) and Whitaker Foundation (H.Y.).

References

1. Honda K, Ohno S, Tanimoto K, et al. (2000) The effects of high magnitude cyclic tensile load on cartilage matrix metabolism in cultured chondrocytes. Eur J Cell Biol 79:601–609
2. Stanford CM, Stevens JW, Brand RA (1995) Cellular deformation reversibly depresses RT-PCR detectable levels of bone-related mRNA. J Biomech 28:1419–1427
3. Cheng B, Kato Y, Zhao S, et al. (2001) PGE(2) is essential for gap junction-mediated intercellular communication between osteocyte-like MLO-Y4 cells in response to mechanical strain. Endocrinology 142:3464–3473
4. You J, Yellowley CE, Donahue HJ, Zhang Y, Chen Q, Jacobs CR (2000) Substrate deformation levels associated with routine physical activity are less stimulatory to bone cells relative to loading-induced oscillatory fluid flow. J Biomech Eng 122:387–393
5. Bancroft GN, Sikavitsas VI, van den Dolder J, et al. (2002) Fluid flow increases mineralized matrix deposition in 3D perfusion culture of marrow stromal osteoblasts in a dose-dependent manner. Proc Natl Acad Sci U S A 99:12600–12605

6. Cukierman E, Pankov R, Stevens DR, Yamada KM (2001) Taking cell-matrix adhesions to the third dimension. Science 294:1708–1712
7. Hotary KB, Alien ED, Brooks PC, Datta NS, Long MW, Weiss SJ (2003) Membrane type 1 matrix metalloproteinase usurps tumor growth control imposed by the three-dimensional extracellular matrix. Cell 114:33–45
8. Cowin SC (1999) Bone poroelasticity. J Biomech 32:217–238
9. Piekarski K, Munro M (1977) Transport mechanism operating between blood supply and osteocytes in long bones. Nature 269:80–82
10. Knothe Tate ML, Steck R, Forwood MR, Niederer P (2000) *In vivo* demonstration of load-induced fluid flow in the rat tibia and its potential implications for processes associated with functional adaptation. J Exp Biol 203 Pt 18:2737–2745
11. Tanaka SM, Li J, Duncan RL, Yokota H, Burr DB, Turner CH (2003) Effects of broad frequency vibration on cultured osteoblasts. J Biomech 36:73–80
12. Chen G, Ushida T, Tateishi T (2001) Poly(DL-lactic-co-glycolic acid) sponge hybridized with collagen microsponges and deposited apatite particulates. J Biomed Mater Res 57:8–14
13. Turner CH, Yoshikawa T, Forwood MR, Sun TC, Burr DB (1995) High frequency components of bone strain in dogs measured during various activities. J Biomech 28:39–44
14. Coleman JC, Hart RT, Owan I, Tankano Y, Burr DB (2002) Characterization of dynamic three-dimensional strain fields in the canine radius. J Biomech 35:1677–1683
15. Fang MA, Kujubu DA, Hahn TJ (1992) The effects of prostaglandin E2, parathyroid hormone, and epidermal growth factor on mitogenesis, signaling, and primary responsegens in UMR 106-01 osteoblast-like cells. Endocrinology 131:2113–2119
16. Wadhwa S, Choudhary S, Voznesensky M, Epstein M, Raisz L, Pilbeam C (2002) Fluid flow induces COX-2 expression in MC3T3-E1 osteoblasts via a PKA signaling pathway. Biochem Biophys Res Commun 297:46–51
17. Yokota H, Goldring MB, Sun HB (2003) CITED2-mediated regulation of MMP-1 and MMP-13 in human chondrocytes under flow shear. J Biol Chem 278:47275–47280
18. Sun HB, Nalim R, Yokota H (2003) Expression and activities of matrix metalloproteinases under oscillatory shear in IL-1-stimulated synovial cells. Connect Tissue Res 44:42–49
19. Kunnel JG, Gilbert JL, Stern PH (2002) *In vitro* mechanical and cellular responses of neonatal mouse bones to loading using a novel micromechanical-testing device. Calcif Tissue Int 71:499–507
20. Owan I, Burr DB, Turner CH, et al. (1997) Mechanotransduction in bone: osteoblasts are more responsive to fluid forces than mechanical strain. Am J Physiol 273:C810–815
21. Kawata A, Mikuni-Takagaki Y (1998) Mechanotransduction in stretched osteocytes—temporal expression of immediate early and other genes. Biochem Biophys Res Commun 246:404–408
22. Sun HB, Yokota H (2001) Messenger-RNA expression of matrix metalloproteinases, tissue inhibitors of metalloproteinases, and transcription factors in rheumatic synovial cells under mechanical stimuli. Bone 28:303–309
23. Yamaguchi S, Yamaguchi M, Yatsuyanagi E, et al. (2002) Cyclic strain stimulates early growth response gene product 1-mediated expression of membrane type 1 matrix metalloproteinase in endothelium. Lab Invest 82:949–956
24. Sun HB, Yokota H (2002) Reduction of cytokine-induced expression and activity of MMP-1 and MMP-13 by mechanical strain in MH7A rheumatoid synovial cells. Matrix Biol 21:263–270
25. Lanyon LE, Goodship AE, Pye CJ, MacFie JH (1982) Mechanically adaptive bone remodelling. J Biomech 15:141–154
26. Rubin CT, Lanyon LE (1985) Regulation of bone mass by mechanical strain magnitude. Calcif Tissue Int 37:411–417
27. Pedersen EA, Akhter MP, Cullen DM, Kimmel DB, Recker RR (1999) Bone response to *in vivo* mechanical loading in C3H/HeJ mice. Calcif Tissue Int 65:41–46
28. Turner CH, Forwood MR, Otter MW (1994) Mechanotransduction in bone: Do bone cells act as sensors of fluid flow? FASEB J 8:875–878
29. Harell A, Dekel S, Binderman I (1977) Biochemical effect of mechanical stress on cultured bone cells. Calcif Tissue Res 22(suppl):202–207
30. Banes AJ, Link GW Jr, Gilbert JW, Tran Son Tay R, Monbureau O (1990) Culturing cells in a mechanically active environment. Am Biotechnol Lab 8:12–22
31. Kaspar D, Seidl W, Neidlinger-Wilke C, Beck A, Claes L, Ignatius A (2002) Proliferation of human-derived osteoblast-like cells depends on the cycle number and frequency of uniaxial strain. J Biomech 35:873–880
32. Reich KM, Gay CV, Frangos JA (1990) Fluid shear stress as a mediator of osteoblast cyclic adenosine monophosphate production. J Cell Physiol 143:100–104
33. Sakai K, Mohtai M, Iwamoto Y (1998) Fluid shear stress increases transforming growth factor beta 1 expression in human osteoblast-like cells: modulation by cation channel blockades. Calcif Tissue Int 63:515–520
34. Nauman EA, Satcher RL, Keaveny TM, Halloran BP, Bikle DD (2001) Osteoblasts respond to pulsatile fluid flow with short-term increases in PGE(2) but no change in mineralization. J Appl Physiol 90:1849–1854
35. Ryder KD, Duncan RL (2001) Parathyroid hormone enhances fluid shear-induced [Ca2+]i signaling in osteoblastic cells through activation of mechanosensitive and voltage-sensitive Ca2+ channels. J Bone Miner Res 16:240–248
36. Duncan RL, Akanbi KA, Farach-Carson MC (1998) Calcium signals and calcium channels in osteoblastic cells. Semin Nephrol 18:178–190
37. McAllister TN, Frangos JA (1999) Steady and transient fluid shear stress stimulate NO release in osteoblasts through distinct biochemical pathways. J Bone Miner Res 14:930–936
38. Granet C, Boutahar N, Vico L, Alexandra C, Lagage-Proust MH (2001) MAPK and SRC-kinases control EGR-1 and NF-kappa B inductions by changes in mechanical environment in osteoblasts. Biochem Biophys Res Commun 284:622–631
39. Yamada KM, Pankov R, Cukierman E (2003) Dimensions and dynamics in integrin function. Braz J Med Biol Res 36:959–966
40. Wolf K, Mazo I, Leung H, et al. (2003) Compensation mechanism in tumor cell migration: mesenchymal-amoeboid transition after blocking of pericellular proteolysis. J Cell Biol 160:267–277
41. Weinbaum S, Cowin SC, Zeng Y (1994) A model for the excitation of osteocytes by mechanical loading-induced bone fluid shear stresses. J Biomech 27:339–360
42. Nalim R, Pekkan K, Sun HB, Yokota H (2004) Oscillating Couette flow for *in vitro* cell loading. J Biomech 37:939–942
43. Shu R, McMullen R, Baumann MJ, McCabe LR (2003) Hydroxyapatite accelerates differentiation and suppresses growth of MC3T3-E1 osteoblasts. J Biomed Mater Res 67A:1196–1204
44. Deligianni DD, Katsala ND, Koutsoukos PG, Missirlis YF (2001) Effect of surface roughness of hydroxyapatite on human bone marrow cell adhesion, proliferation, differentiation and detachment strength. Biomaterials 22:87–96
45. Oreffo RO, Driessens FC, Planell JA, Triffitt JT (1998) Growth and differentiation of human bone marrow os-

teoprogenitors on novel calcium phosphate cements. Biomaterials 19:1845–1854
46. Puleo DA, Holleran LA, Doremus RH, Bizios R (1991) Osteoblast responses to orthopedic implant materials *in vitro*. J Biomed Mater Res 25:711–723
47. Hong JY, Kim YJ, Lee HW, Lee WK, Ko JS, Kim HM (2003) Osteoblastic cell response to thin film of poorly crystalline calcium phosphate apatite formed at low temperatures. Biomaterials 24:2977–2984
48. Nordstrom E, Ohgushi H, Yoshikawa T, Yokobori AT Jr, Yokobori T (1999) Osteogenic differentiation of cultured marrow stromal stem cells on surface of microporous hydroxyapatite based mica composite and macroporous synthetic hydroxyapatite. Biomed Mater Eng 9:21–26
49. Ohgaki M, Kizuki T, Katsura M, Yamashita K (2001) Manipulation of selective cell adhesion and growth by surface charges of electrically polarized hydroxyapatite. J Biomed Mater Res 57:366–373
50. Klein-Nulend J, Roelofsen J, Semeins CM, Bronckers AL, Burger EH (1997) Mechanical stimulation of osteopontin mRNA expression and synthesis in bone cell cultures. J Cell Physiol 170:174–181
51. Roelofsen J, Klein-Nulend J, Burger EH (1995) Mechanical stimulation by intermittent hydrostatic compression promotes bone-specific gene expression *in vitro*. J Biomech 28:1493–1503
52. Cowin SC, Weinbaum S (1998) Strain amplification in the bone mechanosensory system. Am J Med Sci 316:184–188